

**University of California - Davis****UCD-99-13**

# Technihadron Production and Decay at LEP2

Stephen Mrenna<sup>\*</sup>Department of Physics, University of California at Davis  
Davis, CA 95616

February 1, 2008

## Abstract

The simple “straw–man” model of low–scale technicolor contains light color–singlet technihadrons, which mix with the electroweak gauge bosons. We present lepton collider production rates at the parton level, and show that experiments at LEP2 may be sensitive to the presence of technirho and techniomega states with masses 10 – 20 GeV *beyond* the center–of–mass energy because of the mixing. The exact sensitivity depends on several parameters, such as the technipion mass, the technipion mixing angle, and the charge of the technifermions. In an appendix, we describe the implementation of the model into the event generator PYTHIA for particle–level studies at lepton and hadron colliders.

---

<sup>\*</sup>mrenna@physics.ucdavis.edu

## 1 The Technicolor Straw Man Model

Strongly-coupled models of electroweak symmetry breaking are expected to have additional structure beyond the would-be Goldstone bosons that give mass to the  $W$  and  $Z$  bosons. In this study, we predict the lepton-collider production rates at the parton level of the lightest color-singlet technivector mesons  $\rho_T$  and  $\omega_T$  with masses around 200 GeV, which should be relevant to physics studies at LEP2. The basis for this analysis is the “Technicolor Straw Man Model,” or TCSM [1], which consists of a particle spectrum and effective Lagrangian to describe the phenomenology of the lowest-lying states from a more complete theory of dynamical symmetry breaking. The complete theory is expected to contain some of the aspects of technicolor [2], extended technicolor [3], walking technicolor [4], top condensate models and topcolor-assisted technicolor (TC2) [5, 6, 7, 8], and/or multiscale technicolor [9]. Some signatures of low-scale technicolor in the TCSM have been considered at hadron and muon colliders [10]. Here, we address the issue of what can be learned from the LEP2 collider operating at a center-of-mass energy  $\sqrt{s} \simeq 200$  GeV. We concentrate on the challenging case when the  $\rho_T$  and  $\omega_T$  masses are larger than  $\sqrt{s}$ .

In the TCSM, only the lowest-lying bound states of the lightest technifermion doublet,  $(T_U, T_D)$  are considered. The technifermions are assumed to be color singlets and to transform under technicolor  $SU(N_{TC})$  in a fundamental representation, with electric charges  $Q_U$  and  $Q_D$ . The phenomenology considered here depends only on the sum of these charges  $Q \equiv Q_U + Q_D$ . The bound states of the technifermions are the pseudoscalar isotriplet  $\Pi_T^{\pm,0}$  and isosinglet  $\Pi_T^{0\prime}$  mesons, and the vector isotriplet  $\rho_T^{\pm,0}$  and isosinglet  $\omega_T$  mesons. The technihadron mass scale is set by the technipion decay constant  $F_T$ . In TC2 models,  $F_T \simeq F_\pi/\sqrt{N_D}$ , where  $F_\pi = 246$  GeV, and  $N_D$  is the number of electroweak doublets of technifermions. In a specific model,  $N_D \simeq 10$  and  $F_T \simeq 80$  GeV [8]. The interaction states  $\Pi_T$  are admixtures of the electroweak Goldstone bosons  $W_L$  and the mass eigenstates of pseudo-Goldstone technipions  $\pi_T^\pm, \pi_T^0$ :

$$|\Pi_T\rangle = \sin \chi |W_L\rangle + \cos \chi |\pi_T\rangle, \quad (1)$$

where  $\sin \chi = F_T/F_\pi$  ( $\simeq 1/\sqrt{10}$  in the model mentioned above). Similarly,  $|\Pi_T^{0\prime}\rangle = \cos \chi' |\pi_T^{0\prime}\rangle + \dots$ , where  $\chi'$  is another mixing angle and the ellipsis refer to other technipions needed to eliminate the technicolor anomaly from the  $\Pi_T^{0\prime}$  chiral current. If techni-isospin is a good approximate symmetry,  $\rho_T$  and  $\omega_T$ , and, separately,  $\pi_T^0, \pi_T^{0\prime}, \pi_T^\pm$  are nearly degenerate in mass. However,

there may be appreciable  $\pi_T^0 - \pi_T^{0'}$  mixing [10]. If that is the case, the lightest neutral technipions are maximally-mixed  $\bar{T}_U T_U$  and  $\bar{T}_D T_D$  bound states.

### 1.1 Techniscalar decays

Technipion decays are induced mainly by extended technicolor (ETC) interactions which couple them to quarks and leptons like Higgs bosons [3]. With a few exceptions, technipions are expected to decay into the heaviest fermion pairs allowed. One exception is that decays to top quarks are not enhanced, since ETC interactions only generate a few GeV of the top quark mass. Another exception is that the constituents of the isosinglet  $\pi_T^{0'}$  may include colored technifermions as well as color-singlets, so that decays into a pair of gluons are possible. Therefore, the important decay modes are  $\pi_T^+ \rightarrow c\bar{b}, u\bar{b}, c\bar{s}, d\bar{d}$  and  $\tau^+ \nu_\tau$ ;  $\pi_T^0 \rightarrow b\bar{b}, c\bar{c}, \tau^+ \tau^-$ ; and  $\pi_T^{0'} \rightarrow gg, b\bar{b}, c\bar{c}, \tau^+ \tau^-$ . Branching ratios are presented in Fig. 1 for  $\pi_T^0$  (solid lines) and  $\pi_T^{0'}$  (dash-dot lines) using the expressions of Ref. [1] and  $C_f = 1$ , except  $C_t = m_b/m_t$ ,  $C_{\pi_T} = 4/3$ ,  $N_{TC} = 4$ , and  $F_T = 82$  GeV. The  $\pi_T^0$  and  $\pi_T^\pm$  branching ratios are fairly flat as a function of  $M_{\pi_T}$ , while  $\pi_T^{0'}$  shows more variation because of the  $gg$  decay mode.

In addition to these considerations, there may be light topcolor pions present in a realistic theory, and these can mix with the ordinary technipions. The topcolor pions couple preferentially to top quarks, but there can be flavor mixing and instanton effects [11]. The neutral top pion  $\pi_t^0$  can decay  $\rightarrow t\bar{t}$  above threshold;  $\rightarrow t\bar{t}^* \rightarrow tbW$  below threshold;  $\rightarrow t\bar{c}, t\bar{u}$  through mixing;  $\rightarrow b\bar{b}$  through instanton effects; or  $\rightarrow gg$  through a top quark loop. The charged top pion can decay  $\pi_t^+ \rightarrow t\bar{b}$  above threshold;  $\rightarrow t^*\bar{b} \rightarrow b\bar{b}W$  below threshold; or  $\rightarrow b\bar{c}$  (etc.) through mixing. Typical branching ratios for  $\pi_t^0$  and  $\pi_t^\pm$  decays are shown in Fig. 1 (short-dashed lines) with the toppion decay constant set to 82 GeV. For the mass range considered here, only  $\pi_t^0$  decays to  $b\bar{b}$  and  $gg$  final states are important. Note that off-shell decays  $\pi_t^\pm \rightarrow b\bar{b}W$  can be competitive with the mixing-suppressed decay to  $bc$  (the suppression was arbitrarily chosen as  $(.05)^2$  for this plot). In the following, we ignore the complication of technipion–toppion mixing and assume that the technipions decay according to the expectations of the TCSM.

## 1.2 Technivector decays

In the limit that the electroweak gauge couplings  $g, g' \rightarrow 0$ , the isospin-conserving decays of  $\rho_T$  and  $\omega_T$  are fixed by the technipion mixing angle:

$$\begin{aligned}\rho_T &\rightarrow \Pi_T \Pi_T = \cos^2 \chi (\pi_T \pi_T) + 2 \sin \chi \cos \chi (W_L \pi_T) + \sin^2 \chi (W_L W_L); \\ \omega_T &\rightarrow \Pi_T \Pi_T \Pi_T = \cos^3 \chi (\pi_T \pi_T \pi_T) + \dots\end{aligned}\quad (2)$$

Because of the lifting of the technipion masses by the hard technifermion masses, the TCSM assumes the decay  $\omega_T \rightarrow \pi_T \pi_T \pi_T$  are kinematically forbidden. In addition, we do not consider models where  $\omega_T \rightarrow W_L W_L Z_L$  is possible. The isospin violating decay rates obey the relation  $\Gamma(\omega_T \rightarrow \pi_A^+ \pi_B^-) = |\epsilon_{\rho\omega}|^2 \Gamma(\rho_T^0 \rightarrow \pi_A^+ \pi_B^-)$ , where  $\epsilon_{\rho\omega}$  is the isospin-violating  $\rho_T$ - $\omega_T$  mixing amplitude. In QCD,  $|\epsilon_{\rho\omega}| \simeq 5\%$ , so the isospin violating decays in the TCSM are expected to be unimportant.

The technivectors also undergo 2-body decays to transverse gauge bosons and technipions ( $\gamma \pi_T$ ,  $W \pi_T$ , etc.) and fermion-anti-fermion pairs  $f \bar{f}$ . The decay rates to transverse gauge bosons are set by a vector or axial mass parameter,  $M_V$  and  $M_A$ , respectively, which is expected to be of the same order as  $F_T$ , and are proportional to  $\cos^2 \chi$  or  $\cos^2 \chi'$ . Decays where the mother and daughter techniparticle have the same isospin and electric charge are proportional to  $Q^2$ , and the decays to  $Z^0 \pi_T$  are of similar strength as  $\gamma \pi_T$ . The  $\rho_T$  and  $\omega_T$  decay to fermions because of the technifermion couplings to the standard model (SM) gauge bosons. In general, the branching ratios to fermions are small, and the  $\omega_T$  decay rate is proportional to  $Q^2$ .

## 1.3 Direct technipion production

The lightest technimeson states are difficult to produce directly at  $e^+ e^-$  colliders. The process  $e^+ e^- \rightarrow \pi_T^0 \propto \Gamma(\pi_T^0 \rightarrow e^+ e^-) \propto (\frac{m_e}{F_T})^2$  is suppressed by a small coupling, while  $\gamma \gamma \rightarrow \pi_T^0 \propto \Gamma(\pi_T^0 \rightarrow \gamma \gamma)$  is one-loop suppressed. Additionally, the technipions have no tree level couplings to  $W$  or  $Z$ , negating the usual Higgs boson production modes at lepton colliders. The charged technipion can be pair-produced through a virtual photon, but the production rates are not large. For a center-of-mass energy  $\sqrt{s} = 200$  GeV, the production cross section falls as (.169,.115,.063,.024,.011) pb for  $M_{\pi_T^\pm} = (80,85,90,95,97)$  GeV. The SM  $W^+ W^-$  cross section is about 20 pb, and it is problematic whether an excess of events with heavy flavor can be observed above the backgrounds (because of TC2, such a light charged technipion is not constrained by top quark decays). Presently, LEP experiments set a

95% C.L. exclusion on a charged Higgs boson with mass in the range 52–58 GeV [12]. Therefore, we only consider models with technipions heavier than this limit.

#### 1.4 Technivector production

The explicit formulae for the cross sections of the technivector-mediated processes have been presented in Ref. [1]. Unlike the technipions, the technirho and techniomega can have substantial mixing with the SM gauge bosons, and can be produced with electroweak strength. The mixing between  $\gamma, Z$  and  $\rho_T, \omega_T$  is proportional to  $\sqrt{\alpha/\alpha_{\rho_T}}$ , where  $\alpha$  is the fine structure constant and  $\alpha_{\rho_T}$  is the technirho coupling, which is fixed in the TCSM by scaling the ordinary rho coupling by  $N_{TC}$  ( $= 4$  in this analysis). The full expression for the mixing depends also on the masses and widths of the technivectors. In addition,  $\gamma - \omega_T$  and  $Z - \omega_T$  mixing is proportional to  $Q$ .

From the discussion of decay rates above, the technirho and techniomega are also expected to be narrow, which naively reduces the reach of a lepton collider to regions where the center-of-mass energy is close to the resonance mass. However, the resonances are not of the simple, Breit–Wigner form, and the effects of mixing can be seen at lower energies than a few total widths from the resonance mass. On resonance, the production cross sections are substantial ( $\mathcal{O}(\text{nb})$  strength for the models considered here), and a tail may be visible even if the nominal mass of the resonance is 10–20 GeV *above* the collider energy. If the resonance mass is substantially *below* the center-of-mass energy, then the resonance is produced in radiative return events, and should be easily excluded [13].

## 2 Technivector models

To estimate the prospects for observing technivectors at LEP2, we have to fix all of the TCSM parameters. The remaining important parameters are the mass splittings between the vectors and scalars  $\Delta M \equiv M_{\rho_T} - M_{\pi_T}$ , the technipion mixing angle  $\chi$ , and the sum technifermion charge  $Q$ . The choices of model parameters are outlined in Table 1. The vector and axial mass parameters are fixed at  $M_V = M_A = 100$  GeV,  $\sin \chi' = \sin \chi$ , and  $M_\rho = M_\omega$  for simplicity. While the choice is not exhaustive, the models are intended to illustrate basic patterns of signals.

Model 1 has relatively heavy  $\rho_T$  and  $\omega_T$ , and the decays  $\rho_T \rightarrow W_L^+ W_L^-$

Model	$\sin \chi$	$Q$	$M_\rho$ (GeV)	$M_\pi$ (GeV)	$\Gamma_{\rho_T}$ ( $\Gamma_{\omega_T}$ ) (GeV)	Symbol
1	1/3	5/3	210	110	1.36 (.46)	dashes
2	1/3	0	200	110	.33 (.34×10 <sup>-2</sup> )	dots
3	1/3	-1	205	175	.15 (.26×10 <sup>-1</sup> )	dash-dots
4	1	5/3	200	105	7.64 (.44×10 <sup>-1</sup> )	△
5	0	5/3	200	105	0.64 (.43)	+
6	0	5/3	205	100	1.24 (.56)	○
7	0	0	200	80	8.50 (0.23)	×
8	1	0	200	80	7.67 (0)	□

Table 1: The parameters of the TCSM models used in this analysis.

and  $\rightarrow W_L^\pm \pi_T^\mp$  are suppressed by mixing and phase space. The charge  $Q$  is large, so that  $\omega_T$  has a large branching ratio to  $\gamma\pi_T$  and  $f\bar{f}$  final states and a large  $\gamma - \omega_T$  and  $Z - \omega_T$  mixing. Model 2 has a lighter  $\rho_T$  and  $\omega_T$  and  $Q = 0$ , so that the  $\omega_T f\bar{f}$  coupling and  $\gamma/Z - \omega_T$  mixing vanishes. Model 3 has a small mass splitting  $\Delta M$ , so that  $\rho_T \rightarrow W_L^\pm \pi_T^\mp$  is forbidden on-shell, and  $Q = -1$ , which yields similar  $\gamma/Z - \rho_T$  and  $\gamma/Z - \omega_T$  mixing. Model 4 has the maximal coupling to  $W_L^+ W_L^-$ , while Model 5 has the minimal coupling, but  $\rho_T \rightarrow \pi_T^+ \pi_T^-$  is kinematically forbidden on-shell. Model 6 is similar to Model 5, but  $\rho_T \rightarrow \pi_T^+ \pi_T^-$  is allowed on-shell. Finally, Models 7 and 8 have light technipions, with unsuppressed couplings to  $W_L^+ W_L^-$  and  $\pi_T^+ \pi_T^-$ , respectively, but  $Q = 0$  to suppress  $\omega_T f\bar{f}$  couplings and  $\gamma/Z - \omega_T$  mixing. The decay widths for the  $\rho_T$  ( $\omega_T$ ) calculated from these parameters are shown in the next-to-last column of Table 1. The final column shows the symbols used in the figures to denote the Models 1–8.

### 3 Signatures

We concentrate on four basic signatures. The first two, the Drell–Yan production of  $\mu^+\mu^-$  and  $W_L^+ W_L^-$  pair production, contain only SM particles in the final state. The last two contain either two technipions or a technipion and an electroweak gauge boson.

#### 3.1 Drell–Yan

As explained above, the technirho and techniomega couple to final states containing fermion pairs through mixing with  $\gamma$  and  $Z$  bosons. We consider

the the  $\mu^+\mu^-$  final state here, since this avoids the complication of Bhabha scattering. The expected cross sections for the various models as a function of the center-of-mass energy  $\sqrt{s}$  is illustrated in Fig. 2. It is worth noting the sensitivity to resonances with pole masses above the energy  $\sqrt{s}$ , despite the fact that the resonances are narrow. In particular, Model 1, with  $M_{\rho_T} = 210$  GeV and  $\Gamma_{\rho_T} = 1.36$  GeV,<sup>1</sup> has  $S/B = .03, .06, .19$  at  $\sqrt{s} = 160, 180, 200$  GeV in the  $\mu^+\mu^-$  final state, where  $S \equiv \Delta\sigma\mathcal{L}$  is the deviation from the standard model cross section times the integrated luminosity, and  $B$  is the expected number of standard model events. The large values for  $\Delta\sigma$  (even sizeable 50 GeV from the resonance peak) is due to the large charge  $Q = 5/3$  in this model. If  $Q = -1$  ( $Q_U = 0$ ), then  $S/B = .02, .04, .12$  with all other parameters fixed. Likewise, for  $Q = 0$ , which is the limit that the  $\omega_T f\bar{f}$  coupling and  $\gamma/Z - \omega_T$  mixing vanishes, we have  $S/B = .01, .02, .07$ . Far from the resonance peak, measurements of such variations in the overall rate will have important systematic as well as statistical errors, so it is important to have a verification of an effect. Because of the SM quantum numbers (and the energy range considered), there is more sensitivity in the lepton pair final state than in the quark pair, and, for the same set of parameters, the effect in the  $b\bar{b}$  final state is roughly half of that in the  $\mu^+\mu^-$  one. There is also difference in the angular distribution of the decay products because of the interference between the various resonances, but this is not dramatic.

The general feature that the cross section decreases before increasing on the resonance is true even for  $Q < 0$ , since the  $\gamma\gamma, ZZ$  and  $\gamma Z$  components of the inverse propagator are quadratic in  $Q$ . The only models that do not demonstrate a significant effect in the fermion pair final state are those where the technirho is fairly wide and  $Q = 0$ , so that the  $\gamma/Z - \omega_T$  mixing vanishes (Models 7 and 8).<sup>2</sup> In these cases, a substantial signal is expected in the  $\rho_T$ -mediated  $W_L^+ W_L^-$  or  $\pi_T^+ \pi_T^-$  channels.

### 3.2 $W_L^+ W_L^-$

If  $\sin\chi \rightarrow 1$ , the  $\rho_T$  coupling to the  $W_L^+ W_L^-$  final state can be important. This is illustrated in Fig 3, where only models that yield a visible signal are shown. The SM prediction for the  $W^+W^-$  cross section is shown for refer-

---

<sup>1</sup>The input mass parameters for the technivectors are not pole masses, so the peak of the resonance is shifted.

<sup>2</sup>In this extreme case, the techniomega appears to be unreasonably narrow. Small isospin-violating effects will have to be included, but they will not contribute significantly to the  $f\bar{f}$  final state.

ence. Model 4 , with  $\sin \chi = 1$ , has  $S/B = .09, 0.5, 3.8$  at  $\sqrt{s} = 180, 190, 200$  GeV, and Model 8 has a similar behavior. (Note, in this figure, the TCSM signal should be added to the standard model component.) The technirho is fairly wide once the  $W_L^+ W_L^-$  channel is unsuppressed, but there is no theoretical motivation for  $\sin \chi \rightarrow 1$ . On the other hand, there is no realistic theory, yet, so we present these results for completeness. The feature around  $\sqrt{s} = 200$  GeV in Model 4 arises from complicated  $\gamma/Z - \rho_T$  interference. When  $\sin \chi = 1/3$ , the increase in cross section is limited to a region of several GeV around the peak position, since the technirho is much narrower. Clearly, on or near the peak, the effect is a striking increase in the total  $W^+ W^-$  production cross section. Otherwise, the signature is a moderate excess of  $W_L^+ W_L^-$  events on a potentially large background.

### 3.3 $W_L^\pm \pi_T^\mp + \pi_T^+ \pi_T^-$

If the technipion is light enough, the  $\rho_T$  coupling to  $W_L^\pm \pi_T^\mp$  and  $\pi_T^+ \pi_T^-$  as  $\sin \chi \rightarrow 0$  is complementary to the  $W_L^+ W_L^-$  coupling when  $\sin \chi \rightarrow 1$ . This is illustrated by comparing Model 7 in Fig. 4 to Model 8 in Fig. 3, which have large signals in one or the other channel. Both models yield the same  $S/B$  at  $\sqrt{s} = 180$  GeV in their respective channels. Technirho and techniomega couplings to a transverse  $W$  boson and  $\pi_T^\pm$  also arise, but typically at reduced rates compared to  $W_L^\pm \pi_T^\mp$ . Since  $\pi_T^\pm$  decays preferentially to heavy flavor,  $W_L^\pm \pi_T^\mp$  or  $\pi_T^+ \pi_T^-$  production will produce an excess of  $\tau$  or  $b$  and  $c$ -tagged events in the total  $W^+ W^-$  data sample. The experimental sensitivity will be better if  $M_{\pi_T}$  is sufficiently different from  $M_W$ . Note that the off-resonance production rate for  $\pi_T^+ \pi_T^-$  is generally much larger than the usual charged Higgs boson pair production rate discussed earlier.

### 3.4 $\gamma \pi_T^0, \gamma \pi_T^{0'}$

For  $\sin \chi \simeq 0$ , a significant  $\gamma \pi_T^0, \gamma \pi_T^{0'}$  signature can arise.  $Z \pi_T$  production, while possible, is never important relative to  $\gamma \pi_T$  from phase space considerations. The  $\omega_T$  contribution to  $\gamma \pi_T$  can be enhanced significantly if  $Q$  is large, since the  $\gamma/Z - \omega_T$  mixing is proportional to  $Q$ . The expected signal rate is shown in Fig. 5 for the various models. We have not attempted to estimate the backgrounds, which may be prodigious if  $M_{\pi_T} \simeq M_Z$ . However, if  $M_\pi$  is sufficiently different from  $M_Z$ , an off-resonance signal may be observable. The expected final states are  $\gamma b\bar{b}$ ,  $\gamma \tau\tau$  or  $\gamma gg$ . On resonance, the  $\gamma \pi_T$  production rate can be  $\mathcal{O}(100 \text{ pb})$  or larger, and there is still some

rate off resonance even when the  $\rho_T$  and  $\omega_T$  are narrow. Model 1 (with  $Q = 5/3$ ) yields a raw event rate of .18,.54,2.5 pb at  $\sqrt{s} = 180, 190, 200$  GeV. This drops to .06,.18,.90 pb if  $Q = -1$ , and .01,.03,.15 pb for  $Q = 0$ . These three choices for  $Q$  represent  $\omega_T$  domination, equal  $\rho_T$  and  $\omega_T$  contributions, and  $\rho_T$  domination. Model 5, which has  $\sin \chi = 0$  and lighter  $\rho_T$  and  $\omega_T$ , has a raw event rate of .53,2.6,271 pb.

## 4 Discussion and Conclusions

We have presented examples of how several models of low-scale technicolor, in the framework of the TCSM, would manifest themselves at a lepton collider operating near  $\sqrt{s} = 200$  GeV. These can be used to guide searches at LEP2 to discover or constrain TCSM models. The actual limits will depend on the collider energy, the amount of delivered luminosity, and the SM backgrounds in each channel. For reference, it is quite possible that LEP2 will operate at  $\sqrt{s} = 200$  GeV, with  $200 \text{ pb}^{-1}$  of data delivered to each experiment. In this case, each experiment will be sensitive to cross sections near 15 fb in channels which are relatively background free. The production rates shown have no event selection cuts and no effects of initial state radiation. A dedicated analysis at the particle-level is now under way [14] based on the PYTHIA event generator [15]. The details of how to study the TCSM using PYTHIA are included in the Appendix. Here, we review the results of our parton-level study.

On or near resonance, there are substantial signals of technirho and techniomega production in one or more final states. The typical width of the  $\rho_T$  considered is a few tenths to a few GeV, while the  $\omega_T$  ranged from exceedingly narrow up to a few tenths of a GeV. When  $\sin \chi \rightarrow 1$ , the decays  $\rho_T \rightarrow W_L^+ W_L^-$  are unsuppressed. Likewise, when  $\sin \chi \rightarrow 0$ , but  $\rho_T \rightarrow \pi_T^+ \pi_T^-$  is kinematically allowed, a complementary signature arises in the  $\pi_T^+ \pi_T^-$  final state, where  $\pi_T^\pm$  decays predominantly to heavy flavor. For intermediate values of  $\sin \chi$ , decays to  $W_L^\pm \pi_T^\mp$  will occur when kinematically allowed. Also, there can be signals in  $f\bar{f}$  or  $\gamma \pi_T$  final states. These signatures should be unmistakable, since the on-resonance cross sections can be of  $\mathcal{O}(\text{nb})$ . For the same reason, we expect that technivectors with mass significantly below the center-of-mass energy can be easily excluded by searching for radiative return events, but this requires a detailed study [13].

Because of the mixing between the technivector mesons and the electroweak gauge bosons, signatures are not limited to be near the resonance

peak. In particular, the presence of the  $\rho_T$  or  $\omega_T$  may be inferred from a significant decrease in the  $\mu^+\mu^-$  rate, unless the  $\gamma/Z - \omega_T$  mixing is small or the  $\rho_T$  has a width of several GeV. The  $b\bar{b}$  final state would yield a similar effect, but at only about 1/2 the magnitude. Also, the  $\omega_T$  and  $\rho_T$  can mediate the  $\gamma\pi_T$  final state, which may be observable above backgrounds, provided that  $M_{\pi_T}$  is far enough from  $M_Z$ . Event rates of .18 pb are possible at 30 GeV below the resonance peak in the models considered here, depending on the technipion mass, the technifermion charge  $Q$ , and the technipion mixing angle  $\chi$ . Even rates closer to the resonance are much larger.

The choices of TCSM parameters used in this analysis were motivated by the beam energy of LEP2. However, several technicolor-motivated analyses have emerged based on the Run I data sets at the Tevatron [16] that constrain the properties of the color-singlet technirho and techniomega. In general, the technivector masses of the models considered here are beyond the sensitivity of these analyses, except for the techniomega search, which may exclude the models with large  $Q = 5/3$  at the 90% C.L. Therefore, it is expected that LEP2 can set stronger limits than Run I at the Tevatron for  $\rho_T^0$  and  $\omega_T^0$  signatures for certain choices of TCSM parameters.

In conclusion, unless the technipion masses are fairly light compared to the technivector masses (which is not expected due to the enhancement of the hard technifermion masses), or the technipion mixing angle  $\sin \chi \rightarrow 1$  (which is not expected due to the large number of technifermion doublets required in a model with a running coupling), technivector-mediated  $\mu^+\mu^-$  and  $\gamma\pi_T^0, \gamma\pi_T^{0'}$  final states can be studied at LEP2 to discover or constrain simple models of technicolor at collider energies substantially below the technivector masses. The actual limit will depend on a detailed background analysis, but the models studied here yield substantial effects at 10 – 20 GeV below  $M_{\rho_T} = M_{\omega_T}$ . The technirho alone can still produce visible effects in these channels, or (1) the  $W_L^\pm \pi_T^\mp$  final states, if kinematically allowed, (2) the  $W_L^+ W_L^-$  final state, if  $\sin \chi \rightarrow 1$ , or (3) the  $\pi_T^+ \pi_T^-$  final state, if  $\sin \chi \simeq 0$  and the technipion is light.

## Acknowledgements

I thank A. Kounine, G. Landsberg, and K. Lane for useful comments. This work was inspired by the “Strong Dynamics for Run II Workshop” at Fermilab.

## References

- [1] K. Lane, hep-ph/9903369; hep-ph/9903372.
- [2] S. Weinberg, Phys. Rev. **D19**, 1277 (1979); L. Susskind, Phys. Rev. **D20**, 2619 (1979).
- [3] E. Eichten and K. Lane, Phys. Lett. **B90**, 125 (1980).
- [4] B. Holdom, Phys. Rev. **D24**, 1441 (1981); Phys. Lett. **150B**, 301 (1985); T. Appelquist, D. Karabali and L. C. R. Wijewardhana, Phys. Rev. Lett. **57**, 957 (1986); T. Appelquist and L. C. R. Wijewardhana, Phys. Rev. **D36**, 568 (1987); K. Yamawaki, M. Bando and K. Matumoto, Phys. Rev. Lett. **56**, 1335 (1986); T. Akiba and T. Yanagida, Phys. Lett. **169B**, 432 (1986).
- [5] Y. Nambu, Proceedings of the XI International Symposium on Elementary Particle Physics, Kazimierz, Poland, 1988, eds. Z. Adjuk, S. Pokorski and A. Trautmann (World Scientific, Singapore, 1989); Enrico Fermi Institute Report EFI 89-08 (unpublished); V. A. Miransky, M. Tanabashi and K. Yamawaki, Phys. Lett. **221B**, 177 (1989); Mod. Phys. Lett. **A4**, 1043 (1989); W. A. Bardeen, C. T. Hill and M. Lindner, Phys. Rev. **D41**, 1647 (1990).
- [6] C. T. Hill, Phys. Lett. **266B**, 419 (1991) ; S. P. Martin, Phys. Rev. **D45**, 4283 (1992); *ibid* **D46**, 2197 (1992); Nucl. Phys. **B398**, 359 (1993); M. Lindner and D. Ross, Nucl. Phys. **B370**, 30 (1992); R. Bönisch, Phys. Lett. **268B**, 394 (1991); C. T. Hill, D. Kennedy, T. Onogi, H. L. Yu, Phys. Rev. **D47**, 2940 (1993).
- [7] C. T. Hill, Phys. Lett. **345B**, 483 (1995).
- [8] K. Lane and E. Eichten, Phys. Lett. **B352**, 382 (1995) ; K. Lane, Phys. Rev. **D54**, 2204 (1996); K. Lane, Phys. Lett. **B433**, 96 (1998).
- [9] K. Lane and E. Eichten, Phys. Lett. **B222**, 274 (1989); K. Lane and M. V. Ramana, Phys. Rev. **D44**, 2678 (1991).
- [10] E. Eichten and K. Lane, Phys. Lett. **B388**, 803 (1996); E. Eichten, K. Lane and J. Womersley, Phys. Lett. **B405**, 305 (1997); E. Eichten, K. Lane and J. Womersley, Phys. Rev. Lett. **80**, 5489 (1998); S. Mrenna and J. Womersley, Phys. Lett. **B451**, 155 (1999).

- [11] G. Burdman, hep-ph/9611265.
- [12] R. Barate *et al.* [ALEPH Collaboration], Phys. Lett. **B418**, 419 (1998); P. Abreu *et al.* [DELPHI Collaboration], CERN-EP-99-077; M. Acciarri *et al.* [L3 Collaboration], Phys. Lett. **B446**, 368 (1999); K. Ackerstaff *et al.* [OPAL Collaboration], Phys. Lett. **B426**, 180 (1998).
- [13] Yu. Gershtein, S. Kesisoglou, G. Landsberg, paper in preparation.
- [14] A. Kunin, paper in preparation.
- [15] T. Sjostrand, Comput. Phys. Commun. **82**, 74 (1994).
- [16] T. Affolder *et al.* [CDF Collaboration], FERMILAB-PUB-99-141-E; F. Abe *et al.* [CDF Collaboration], hep-ex/9810031.

## Appendix

The simulation of the production and decays of technicolor particles has been substantially upgraded in PYTHIA v6.126, which is available at moose.ucdavis.edu/mrenna, along with documentation.

The full set of processes are:

```
* Drell--Yan (ETC == Extended TechniColor)
194   f+fbar -> f'+fbar' (ETC)
195   f+fbar' -> f"+fbar'' (ETC)
```

The final state fermions are  $e^+e^-$  and  $e^\pm\nu_e$ , respectively, which can be changed through the parameters KFPR(194,1) and KFPR(195,1), respectively.

<pre>* techni_rho0/omega 361   f + fbar -&gt; W_L+ W_L- 362   f + fbar -&gt; W_L+/- pi_T-/ 363   f + fbar -&gt; pi_T+ pi_T- 364   f + fbar -&gt; gamma pi_T0 365   f + fbar -&gt; gamma pi_T0' 366   f + fbar -&gt; Z0 pi_T0 367   f + fbar -&gt; Z0 pi_T0' 368   f + fbar -&gt; W+/- pi_T-/+</pre>	<pre>* charged techni_rho 370   f + fbar' -&gt; W_L+/- Z_L0 371   f + fbar' -&gt; W_L+/- pi_T0 372   f + fbar' -&gt; pi_T+/- Z_L0 373   f + fbar' -&gt; pi_T+/- pi_T0 374   f + fbar' -&gt; gamma pi_T+/- Z0 375   f + fbar' -&gt; Z0 pi_T+/- pi_T0 376   f + fbar' -&gt; W+/- pi_T0 377   f + fbar' -&gt; W+/- pi_T0'</pre>
---	--

All of the processes from 361 to 377 can be accessed at once by setting MSEL=50.

The production and decay rates depend on several "Straw Man" technicolor parameters ( $D$  denotes the default value of a parameter):

```
* Techniparticle masses
PMAS(51,1) (D=110.0 GeV) neutral techni_pi mass
PMAS(52,1) (D=110.0 GeV) charged techni_pi mass
PMAS(53,1) (D=110.0 GeV) neutral techni_pi' mass
PMAS(54,1) (D=210.0 GeV) neutral techni_rho mass
PMAS(55,1) (D=210.0 GeV) charged techni_rho mass
PMAS(56,1) (D=210.0 GeV) techni_omega mass
```

Note: the rho and omega masses are not pole masses

```
* Lagrangian parameters
PARP(141) (D= 0.33333) $|\sin\chi|$, the mixing angle between
    technipion interaction and mass eigenstates
PARP(142) (D=82.0000 GeV) F_T, the technipion decay constant
PARP(143) (D= 1.3333) Q_U, charge of up-type technifermion; the
    down-type technifermion has a charge Q_D=Q_U-1
PARP(144) (D= 4.0000) N_TC, number of technicolors
PARP(145) (D= 1.0000) C_c, coefficient of the technipion decays to charm
PARP(146) (D= 1.0000) C_b, coefficient of the technipion decays to bottom
PARP(147) (D= 0.0182) C_t, coefficient of the technipion decays to top
PARP(148) (D= 1.0000) C_tau, coefficient of the technipion decays to tau
PARP(149) (D=0.00000) C_pi, coefficient of technipion decays to gg
PARP(150) (D=1.33333) C_pi', coefficient of technipion' decays to gg
PARJ(172) (D=200.000 GeV) M_V, vector mass parameter for technivector
    decays to transverse gauge bosons and technipions
PARJ(173) (D=200.000 GeV) M_A, axial mass parameter
PARJ(174) (D=0.33300) $|\sin\chi'|$, the mixing angle between
    the technipion' interaction and mass eigenstates
PARJ(175) (D=0.05000) isospin violating technirho/techniomega mixing
    amplitude
```

Note, the decays products of the  $W$  and  $Z$  bosons are distributed according to phase space, regardless of their designation as  $W_L/Z_L$  or transverse gauge bosons. The exact meaning of longitudinal or transverse polarizations in this case requires more thought.

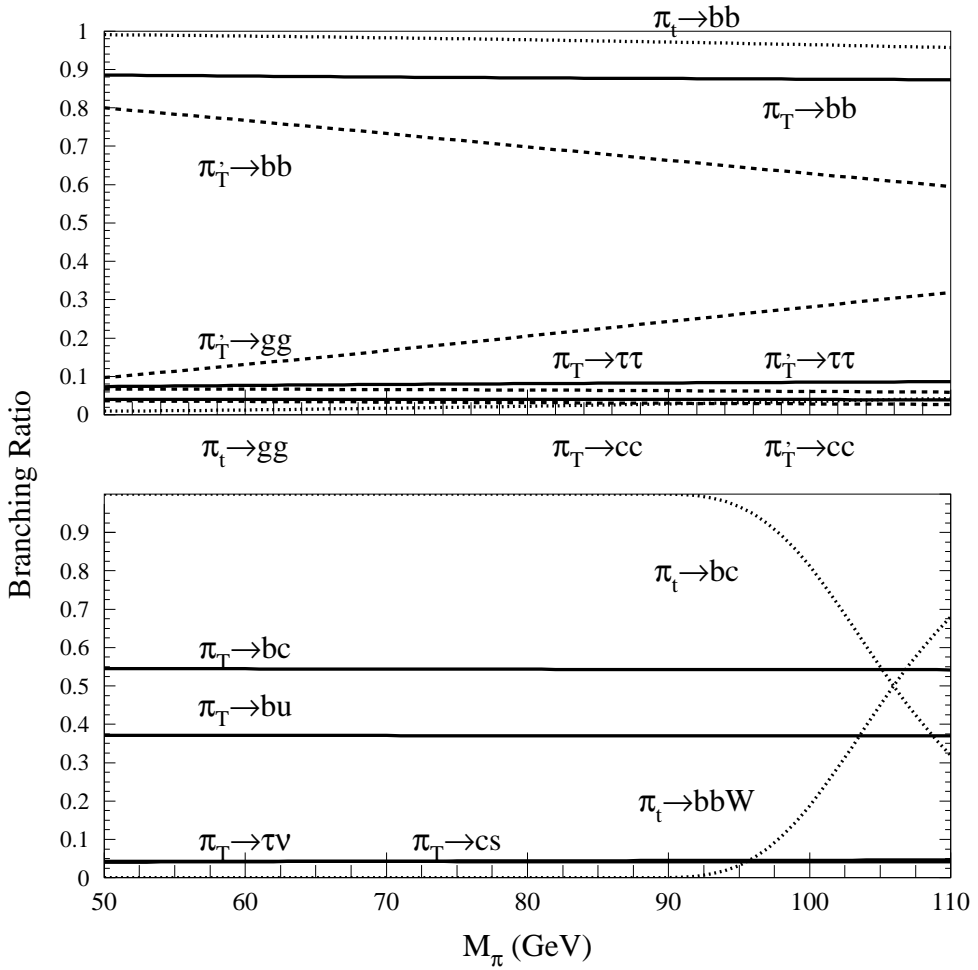


Figure 1: Comparison of different technipion and toppion branching ratios. Decays of  $\pi_T^0$ ,  $\pi_T^{0\prime}$ , and  $\pi_t^0$  are illustrated in the upper part, while  $\pi_T^\pm$  and  $\pi_t^\pm$  are shown in the lower part. The model assumptions are described in the text.

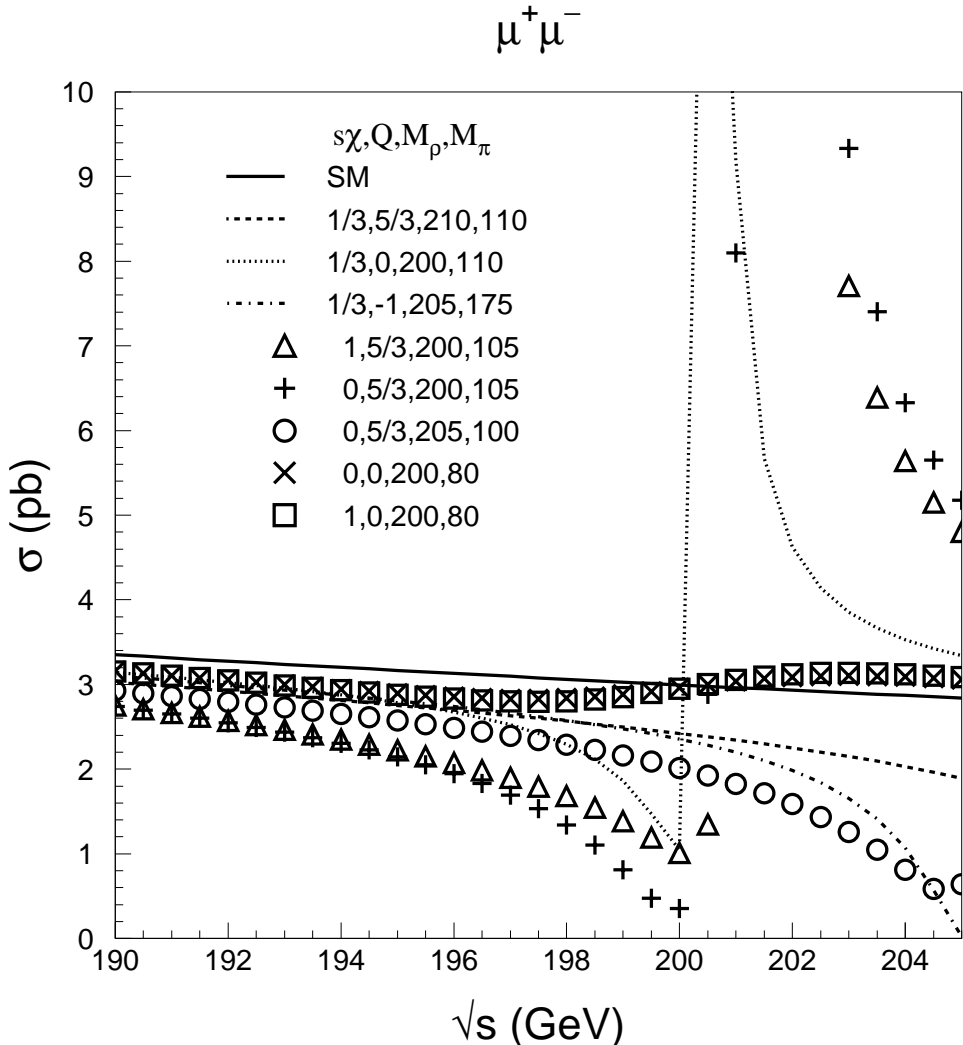


Figure 2: Signatures of TCSM in the final state  $\mu^+ \mu^-$  at an  $e^+ e^-$  collider with center of mass energy  $\sqrt{s}$ . The standard model prediction is shown as the solid (straight) line.

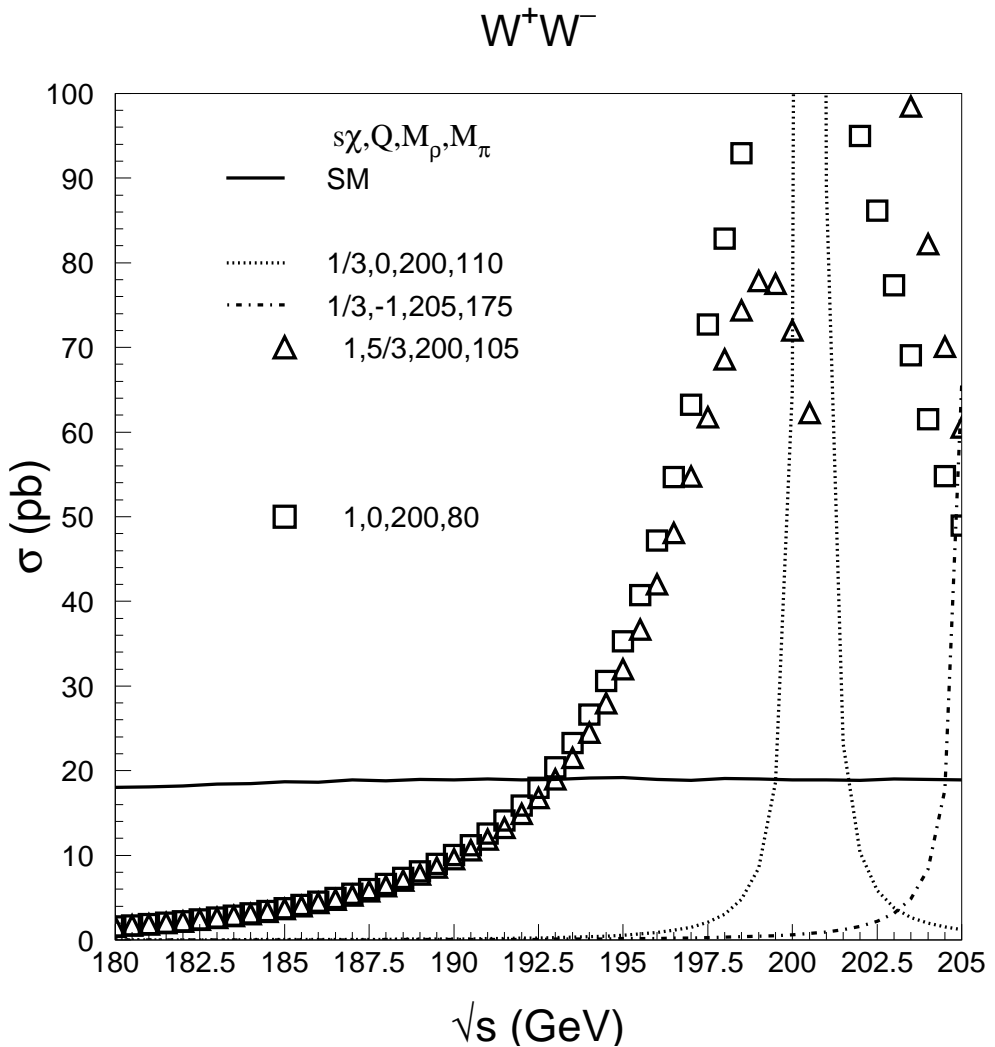


Figure 3: Same as Fig. 2, except for the  $W^+W^-$  final state. The TCSM contribution should be added to the standard model prediction shown.

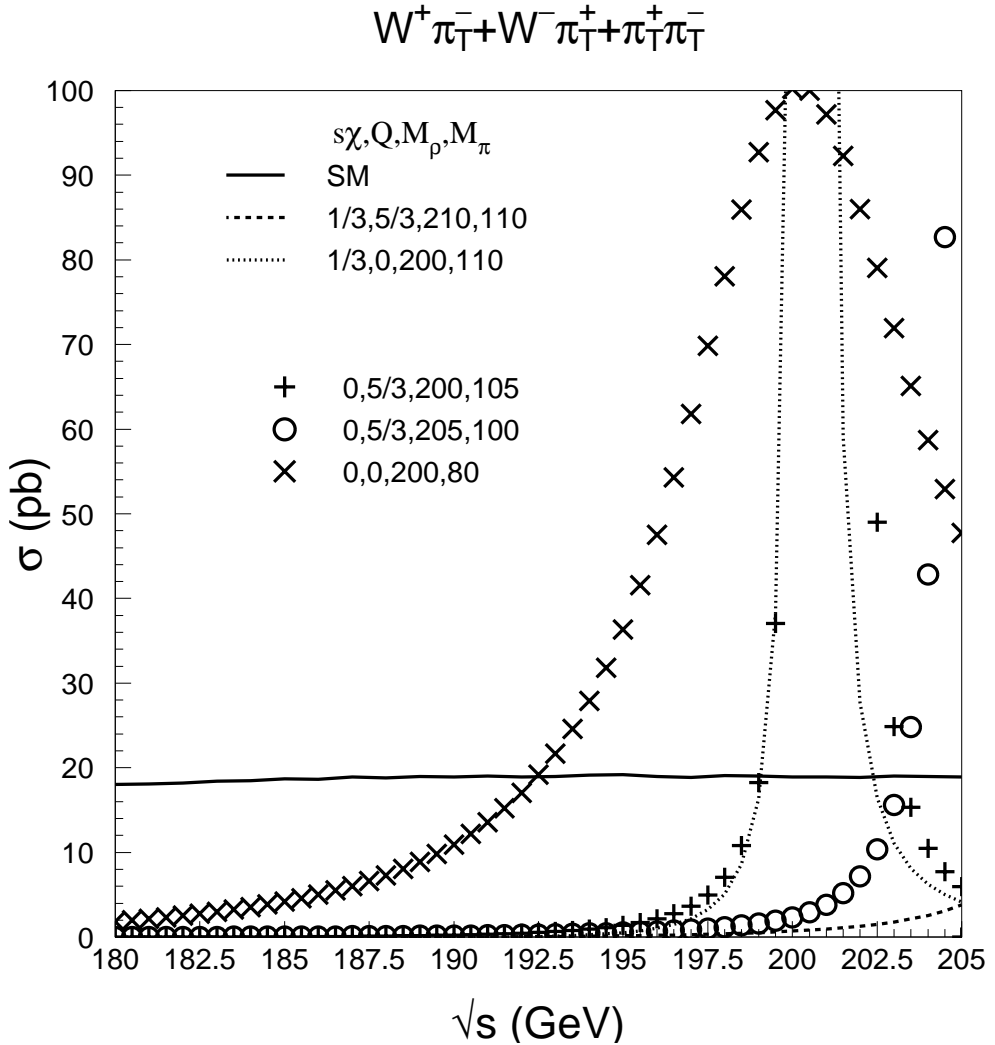


Figure 4: Same as Fig. 3, except for the final state  $W^\pm \pi_T^\mp$  and  $\pi_T^\pm \pi_T^\mp$ . The standard model prediction for  $W^+ W^-$  is shown as the solid line. The TCSM contribution prefers final states containing heavy flavor.

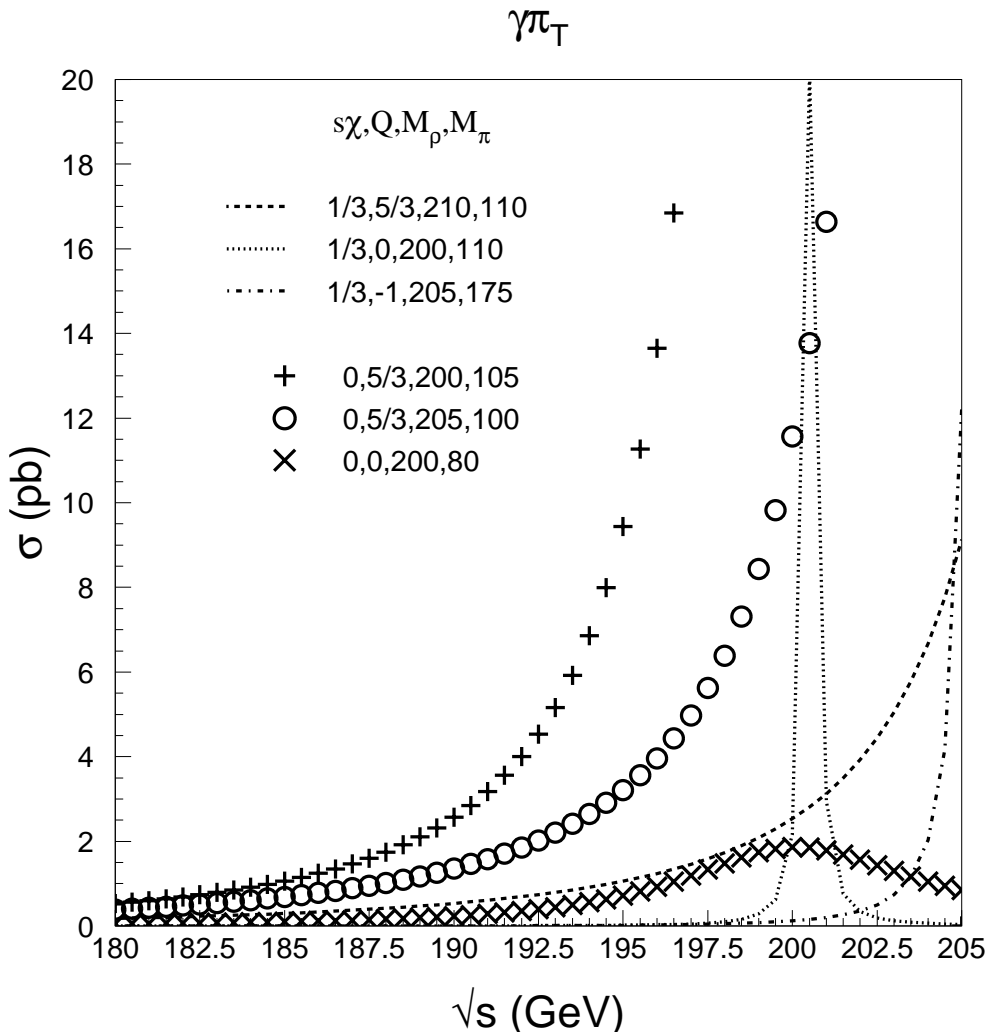


Figure 5: Same as Fig. 3, except for the final state  $\gamma\pi_T^0$  and  $\gamma\pi_T^{0'}$ . The  $\pi_T$  decays preferentially to heavy flavor or  $gg$ .